Ground Effect Flight Transit (GEFT) – Approaches to Design

Galen J. Suppes, PhD, P.E.
Chief Engineer
HS-Drone, LLC
Charlottesville, VA 22911
Email: suppesg@hs-drone.com
ORCiD: 0000-0002-3076-4955

Adam B. Suppes, PhD
Senior Research Engineer
HS-Drone, LLC
Charlottesville, VA, 22911
Email: asuppes@seas.upenn.edu
ORCiD: 0009-0007-5719-7907

Word count: 5623 + 3 tables

Submitted July 30, 2024

Abstract

Preliminary digital prototypes of ground-effect aircraft using a hovercraft-like cavities are able to achieve lift-drag ratio (L/D) efficiencies in excess of 60, which is 4X typical airliners. Preferred speeds are 90 to 300 mph. The highest efficiencies are possible when flying with low clearance to the ground, as is practical with ground-effect flight over railway tracks and highways. Similar efficiencies are attainable over water with larger aircraft. This paper evaluates surrogate airfoil models (i.e., flat plate and simple cambers) toward better understanding how to design ground-effect aircraft suitable for a wide range of applications at L/D efficiencies in excess of 50. Three physical principles identify how to generate lift forces, and three additional principles form the basis for ground-effect aircraft design. Greater than 200% increases in efficiencies are possible in many applications versus the best available alternatives, enabling major strides in: a) zero-carbon emission transit, b) increased transit reliability, c) increased safety, d) low-cost rapid implementation, e) reduced annualized infrastructure costs, and f) reduced transit congestion.

Introduction

Multiple paradigms have crippled the evolution of aircraft for over a century. Foremost among these paradigms are theories of flight that attribute aerodynamic lift to either the turning of air or the simple tradeoff of pressure with velocity. Also, paradigms systematically characterize vehicles with hovercraft-like appearances as being inefficient and of limited application.

The persistence of these paradigms can be attributed to: a) the lack of an accurate simple explanation of aerodynamic lift to displace erroneous explanations, and b) the unknown opportunity costs from failing to use better aircraft platforms. This paper uses three well-founded principles in physics to elucidate how air flow is transformed to aerodynamic lift; three additional principles identify how to achieve high lift-drag ratios (L/D) in aircraft design.

Instant research and development are on a "Ground Effect Flight Transit" (GEFT) lifting-body design that uses a hovercraft-like compartment to systematically achieve L/D efficiencies in excess of 50. Performances are validated with simulation of performances of digital prototypes.

Background

Flight Efficiency – Key benchmarks on flight efficiency are: airliners at L/D ≈ 15, the B1 bomber at L/D ≈ 21, and high aspect ratio gliders at L/D ≈ 60. These benchmarks verify that passenger aircraft can achieve higher flight efficiencies than currently used; however, practical issues hinder these advances.[1-5] The B1 bomber platform is more expensive to build and absent key passive flight stability qualities. The high aspect ratio wings of highly-efficient gliders lack structural capacity to support large passenger cabins. And so, while higher flight efficiencies are fundamentally possible, practical constraints have limited commercial applications in contemporary airframes. Ground effect aircraft use the ground to block losses of lift pressure to attain higher efficiency.[6-8]

Airfoil studies are a common starting point in lifting-body design; where by definition, an airfoil is a 2D cross-section of a lifting body around which air flows. Today's computational fluid dynamics (CFD) simulators are able to provide accurate lift, drag, and L/D characteristics on airfoils. Decades of CFD studies have identified a few airfoils capable of achieving L/D > 50, and occasionally >100.

The 2D studies do not account for lateral loss of lift pressures; hence, the higher benchmark efficiencies are only achieved at high aspect ratios. Winglets are commonly used to reduced lateral loss of lift pressures.

2D simulations in ground-effect flight can systematically achieve L/D > 50 by: a) using lower surfaces that constrict flow between the aircraft and ground on trailing edges, b) having an "effective" lower surface pitch between 0.1° and 1°, and c) having a low-profile upper surface. Within these design constraints, the ground blocks downward loss of lift pressures, oncoming air's dynamic pressure forms higher pressure

throughout the lower surface, and the low pitch allows the higher pressures to generate lift with minimal form drag. Earlier work has demonstrated that L/D in excess of 100 can systematically be achieved with optimization of upper surfaces and distributed propulsion.[9]

In the transformation of 2D performance to 3D digital prototypes, fences along the sides of the lower surface operating with low clearance with the ground readily bock lateral losses of lift pressures with systematic approaches enabling L/D > 40, often in excess of 60. [10] The smooth upper surfaces of rail tracks and highways allows flight with low clearance. This is the first of a sequence of design heuristics identified in a recently filed international patent. [11] The Results section of instant paper expands on the details of the design heuristics.

The CFD methods of this paper are recognized as accurate in estimating performances. [12-14] In fact, digital prototypes are now being used to attain FAA approval without building physical prototypes.[15]

Scientific Rigor – Aerodynamic lift is created by lift pressures, which are higher pressures on lower surfaces and lower pressures on upper surfaces.[16, 17] The following six principles of physics provide explanations of how to convert air flow to lift pressures:

Principle 1. Air velocities impacting surfaces increase surface pressures.

Principle 2. Air velocities diverging from surfaces decrease surface pressures (by creating voids).

Principle 3. Air flows from higher to lower pressures (at the speed of sound); this pressure-driven flow joins with other air flows to form complex streamlines.

Principle 4. The L/D of a section of an airplane surface is approximately equal to 57° divided by the pitch of the surface in degrees for lower surfaces and -57° divided by the pitch for upper surfaces. The pitch angle is relative to horizontal with the nose up as positive.

Principle 5. Surfaces can be used to block loss of lift pressures leading to increased L/D. Example surfaces are winglets on wings and fences under lifting bodies.

Principle 6. For a ground-effect aircraft with properly-designed lower fenced cavity, 3D CFD estimates of cavity lift pressures are able to approach 2D estimates, enabling 2D airfoil simulations to accurately predict actual performances in many applications.

The continuum-level Principles 1-4 are validated on the discrete level of gas molecules through the following restatements in terms of the kinetic theory of gases:

1. Air molecules having random translational directions have increased velocities relative to an approaching airfoil; therefore, the momentum of the molecules relative to the leading edge are increased by a value proportional to the approach speed with a corresponding increase in force caused by the impact of those molecules on leading surfaces. Stated in terms of continuum mechanics, *impacting flow causes higher pressures*.

2. In the absence of translational movement of air molecules, an airfoil would create a perfect vacuum in its wake—similar to the way a snowplow leaves a cleared snow path in its wake. In practice, gas molecules flow into the wake and convert that “perfect vacuum” into a lower pressure region. Stated in terms of continuum mechanics, *diverging flow causes lower pressures*.
3. At room temperature, gas molecules translate 500 m/sec in random directions; the speed of sound in a gas is 340 m/sec which is basically a conversion from random to directional transit. Thus, gases have a net flow through pressure gradients at about the speed of sound. Stated in terms of continuum mechanics, *air flows from higher to lower pressures at the speed of sound*.
4. Atomic interactions with a surface are expressed as lift and form drag based on the pitch of that surface.

These qualitative verifications can become quantitative through Monte Carlo simulation which is computationally intensive and outside the scope of this paper.[18-21] The continuum and discrete mechanics explanations are mutually verifying; and as presented in instant paper, the explanations accurately extrapolate. Other work identifies how to identify sources of lost work toward further, improved understanding.

New Ground-Effect Planform – GEFT is a new ground-effect aircraft platform where a vehicle lower surface with a trailing flap and side fences describes a "cavity", and a well-designed cavity expresses higher pressures throughout the lower surface. One design criterion for that cavity is to maximize the lift are per fence/flap perimeter area which suggests near-square area. However, applications over railway tracks dictates a rectangular area as consistent with railcar design. The platform of Figure 1 emerges with the planform of Figure 2d as a preferred design.

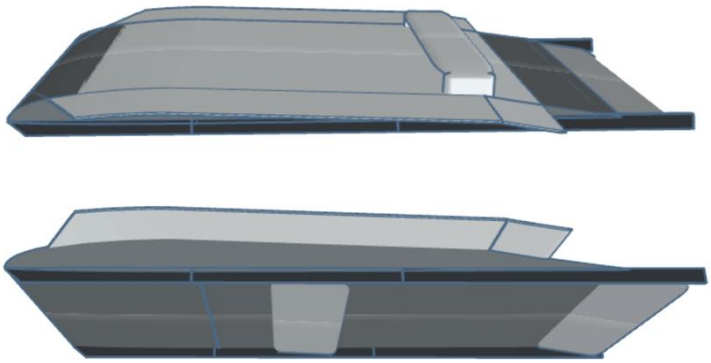

Figure 1. Digital prototype illustrating innovations.

An artifact of recognized ground-effect vehicle planforms 2a-2c is a high reliance on lift generation from wings. Instant paper has placed little to zero emphasis on lateral-extending wings. Optimal lateral-extending wings will increase lift and increase the free-flight L/D.

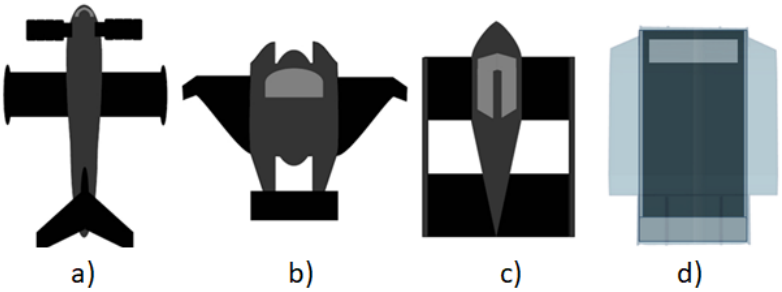

Figure 2. Planforms of a) USSR ekranoplan (1980's), b) Airfish 8 (2024), c) Regent (2024), and d) GEFT (2024).

The GEFT planform resembles a hovercraft; however, it is able to achieve much higher efficiencies than hovercraft and is able to achieve free flight. Two achievements of the GEFT prototype over alternative high-efficiency aircraft are:

- Achieving a L/D greater than 60 for a digital prototype.
- Achieving the ultra-high efficiencies in a vehicle having an aspect ratio less than 1.0.

The airfoil design of these earlier studies (see Figure 3) is the starting point of GEFT lifting-body designs of this paper. Figures 4 and 5 summarize 2D airfoil studies for this early design.[9]. Figure 6 compares the L/D performance of the 2D airfoils to the digital prototypes while Figure 7 identifies how the cavity pressure of 3D prototype approaches the cavity pressure 2D simulations which substantiates Principle 6.

Whereas hovercraft have a design criterion to minimize loss of air at all edges, ground-effect flight has a design criterion of maximizing L/D where pressure is generated by oncoming air's dynamic pressure.

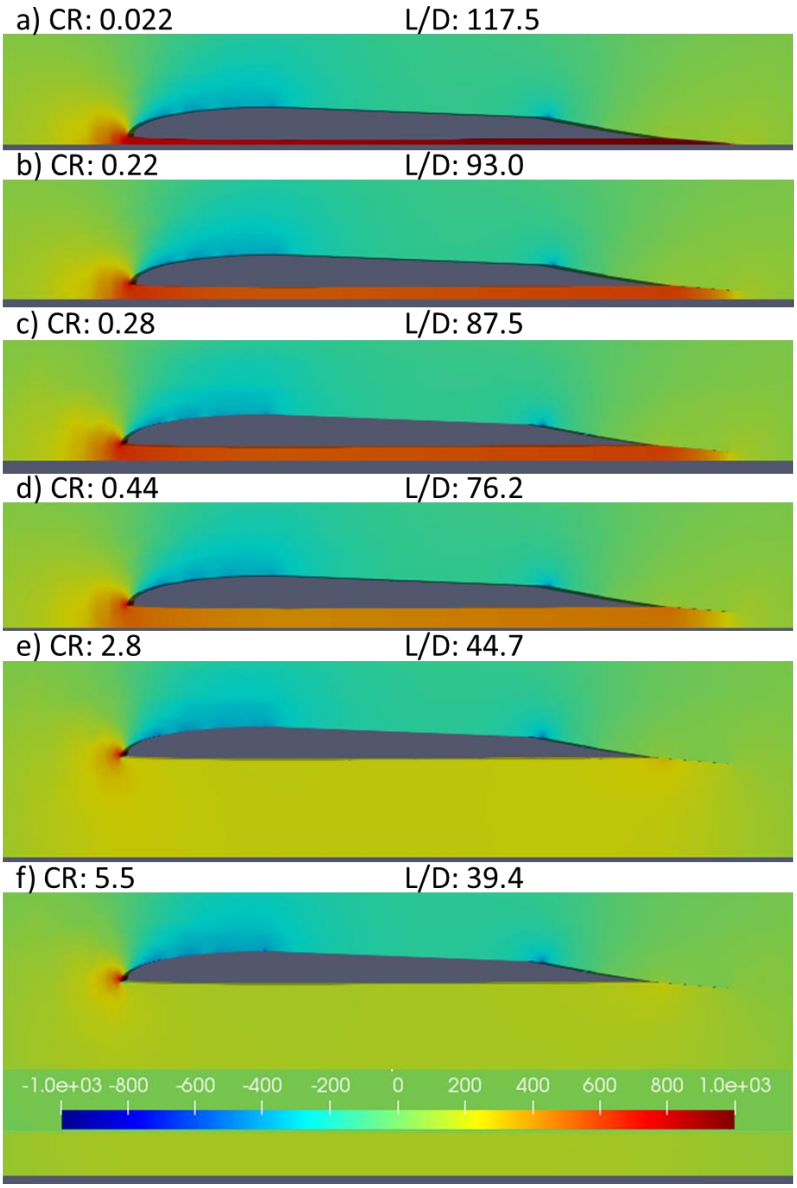

Figure 3. Pressure profiles of early airfoils (Airfoil A) as a function of gap ratio (i.e., ratio of gap with ground to airfoil thickness).

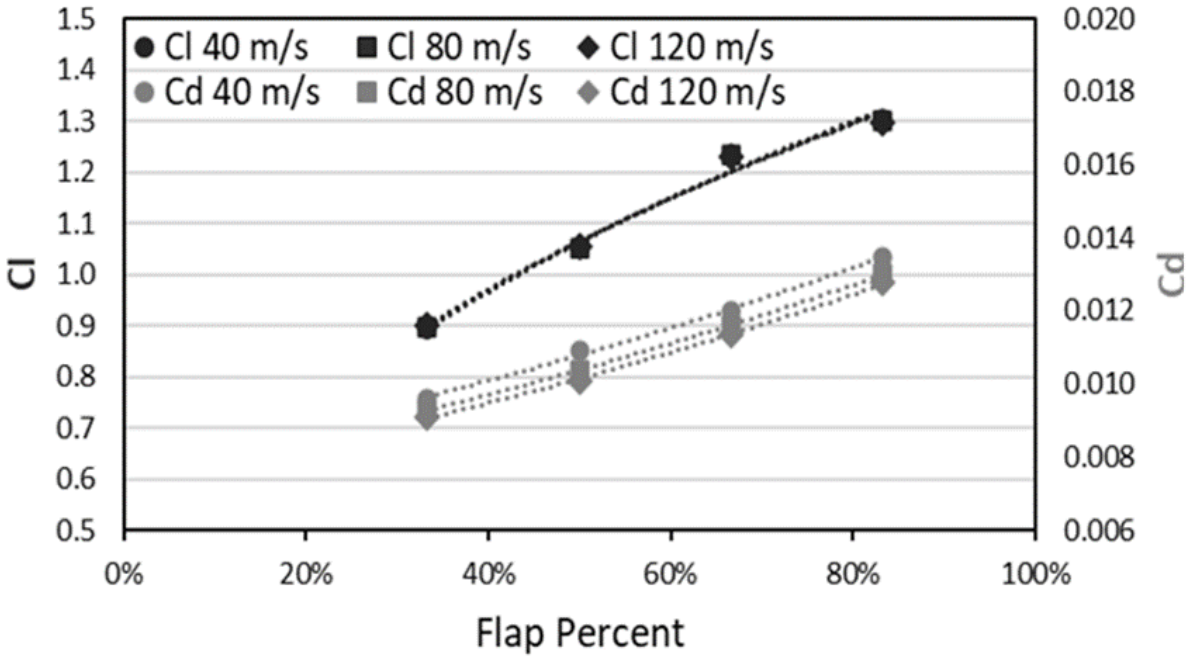

Figure 4. Impact of flap on lift and drag coefficients. Flap fill percent is the downward extension of the flap divided by the downward extension of the fence.

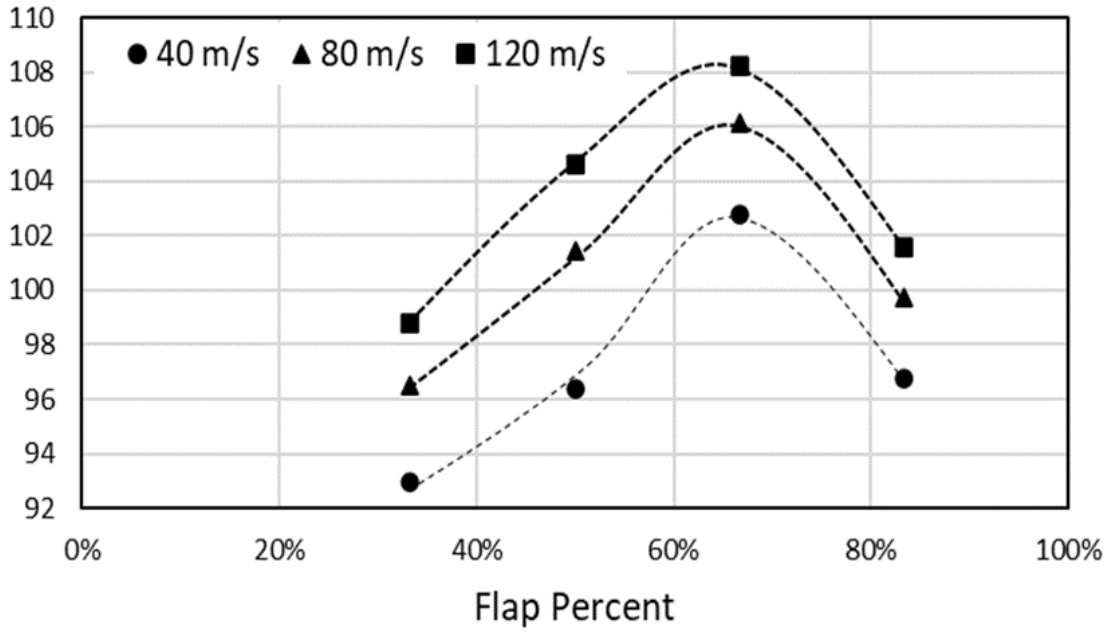

Figure 5. Impact of flap on L/D.

The lateral losses of lift pressures, which is not considered in 2D simulations, are detrimental to L/D performance. A design constraint is to block the losses with a minimum in drag; this translates to longitudinally extending fences where a lower cavity is defined on the sides by fences and on the trailing edge by a flap (see Figure 1). Figure 6 illustrates how the pressure in the cavity of a 3D prototype approaches the 2D

performance as the effectiveness of the fence increases with decreasing clearance ratios.

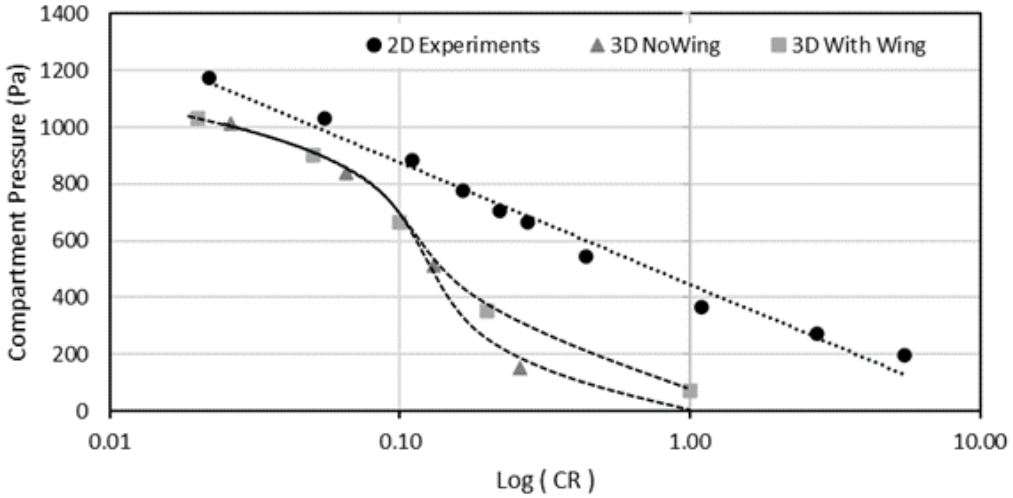

Figure 6. Impact of clearance ratio on average cavity pressure.

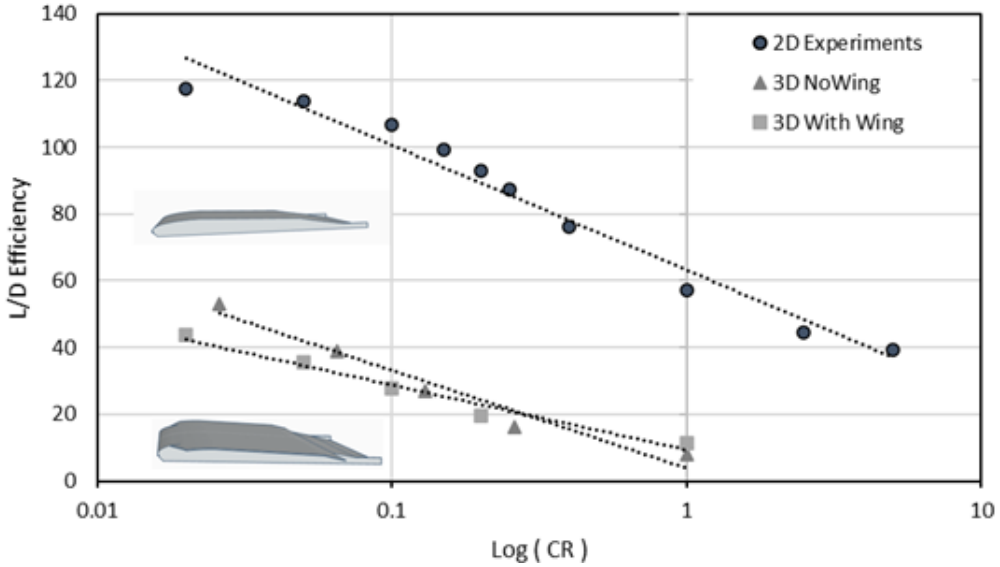

Figure 7. Impact of clearance ratio on L/D Efficiency.

Figure 7 identifies how L/D correlates with the fence height. Whereas the L/D increases with decreasing CR, a fence can be used to move the lower side of the vehicle further from the ground; replacing the vehicle's lower surface with fences that can extend or retract in response to obstacles and as control surfaces. Figure 8 illustrates an optimal extend of fence extension is typically exhibited.

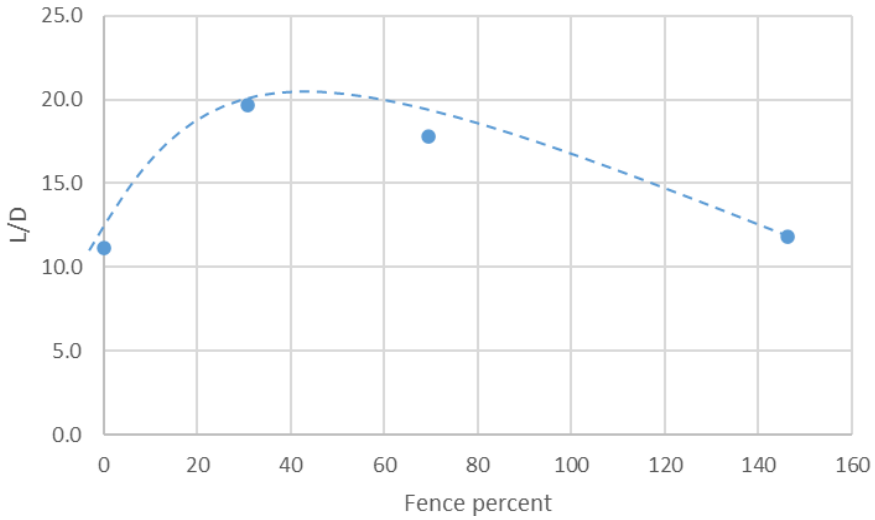

Figure 8. Fence percent is fence height as a percent of airfoil thickness. Data are at a CR = 0.2 and where the bottom of the flap is even with the bottom of the fence. Simulations are 3D, as are all simulations that take into account fences. The correlation is specific to the airfoil of the 3D simulations.

Lift-Span Tech – TRB paper TRBAM-24-04060 of the 2024 Transportation Research Board Annual meeting introduced many of the topics of the current paper, including Lift-Span Tech in Table 1 of that paper. [22] The results of that paper suggest that, in the pursuit of L/D efficiencies greater than 30, distributed propulsion must be properly implemented. The authors' 2023 paper on distributed propulsion teaches toward the use of upper-surface trailing section propulsion to maximize L/D efficiency. Figure 9 and Table 1 illustrate the use of that that propulsion and summarizes the data on which Lift-Span Tech was founded.

Table 1. Conditions of Figure 9 Lift Span simulations.

		-1° Lift Span			4° Lift Span		
FS (m/s)	S (m^4/s^2)	C_l	C_d	L/D	C_l	C_d	L/D
40	0	0.251	0.0338	7.4	0.339	0.0219	15.5
40	20	0.527	0.0157	33.5	0.477	0.0186	25.6
40	40	0.607	0.0092	65.8	0.548	0.0163	33.6

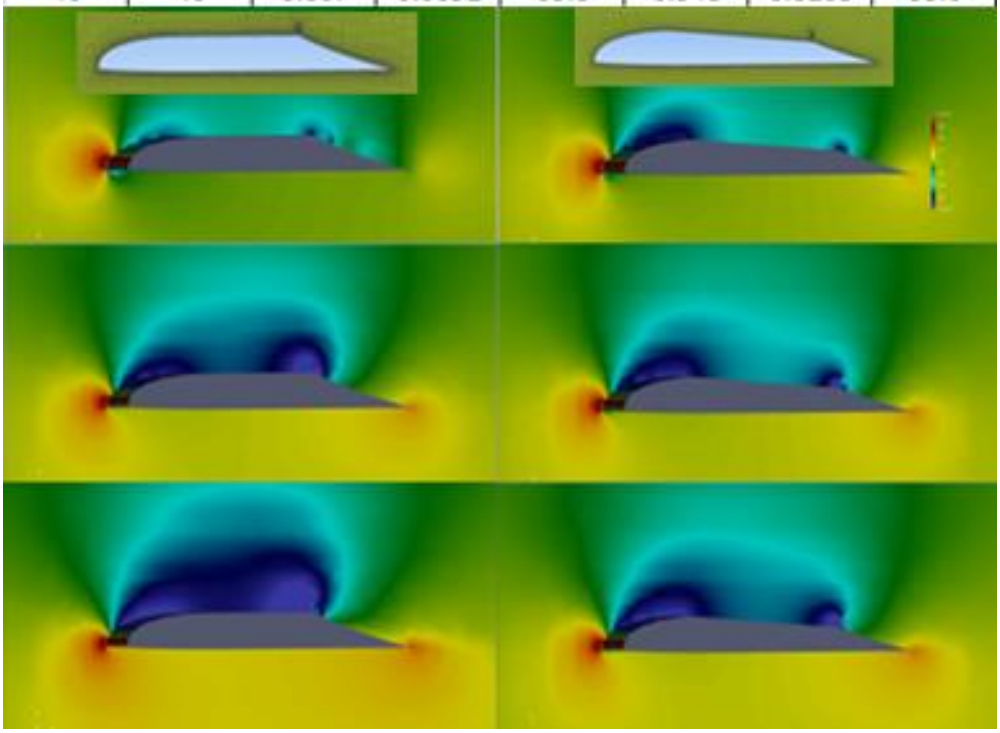

Figure 9. Impact of Lift Span pitch on pressure profiles and L/D of a prototype airfoil. S is propulsor power setting. The pressure scale is relative to free stream pressure with zero at lime-green, red is the highest pressure, and blue is lowest pressure.

Figure 9 data illustrates how a lower pitch at the surface in front of a trailing section propulsor is preferred at the high-power cruising condition while a higher pitch is preferred for low-power gliding or descent. For this paper, only the cruising configuration is considered with the pitch on the mid-chord upper surface of the airfoil and 3D prototypes set at zero.

Methods

Digital Experiments - OpenFoam and Simflow CFD software were used to simulate digital prototypes prepared as STL files. Two-dimensional (2D) simulations were used to identify trends in performance while 3D simulations were performed on the final prototypes. Unless otherwise reported, the scale chord of the STLs were 1 m, the fluid was air at 1 atm pressure, and the free stream velocity was 40 m/s.

The ground was simulated as a lower boundary condition having a velocity equal to the free stream air. Propulsion sources were simulated as cubical geometries that generated horizontal velocities based on the power setting.

Results from CFD simulations (i.e., experiments) include: lift coefficients (C_l), drag coefficients (C_d), L/D (equal to C_l/C_d), pressure profile images, and velocity profile images. Flow around wheels on the vehicle is not considered under the assumption that air flow can be streamlined between fences and wheels.

All pressure profiles of this paper use a pressure color plat with equal positive and negative magnitudes. This allows conclusions to be drawn from pressure profiles without attention to the magnitude. Vivid red is always higher pressure (relative to free stream pressure), vivid blue is lower pressure, and lime green is free stream pressure. The pressure is reported as P/ρ in units of m^2/s^2.

Approach of This Paper – Figure 10 summarizes the airfoils used in this study. Flat plate and cambered airfoils were used to gain a better understanding of the design features impacting performance. The thicker fuselage series starts with a version of the Figure 9 airfoil with an upper-surface mid-chord section having a pitch of zero. The evolution of that airfoil reflects a learning or re-learning of the key design features necessary to gain high L/D efficiency.

A prominent method of design in the aircraft industry is to incrementally change proven designs, and due to the complexity of these designs it is difficult to gain a fundamental understanding from related design studies. The current work emphasizes the study of simpler airfoils toward improved understanding. For the GEFT design, relatively simple designs often offer high L/D efficiency in the right applications.

Another feature of the current work that is not common is past reporting of research is the use of Sources to simulate the impact of lower and higher pressures generated by a fan, propeller, or jet engine on lift, drag, and L/D.

The lower image of Figure 10 illustrates terminology as used in the Results and Discussion.

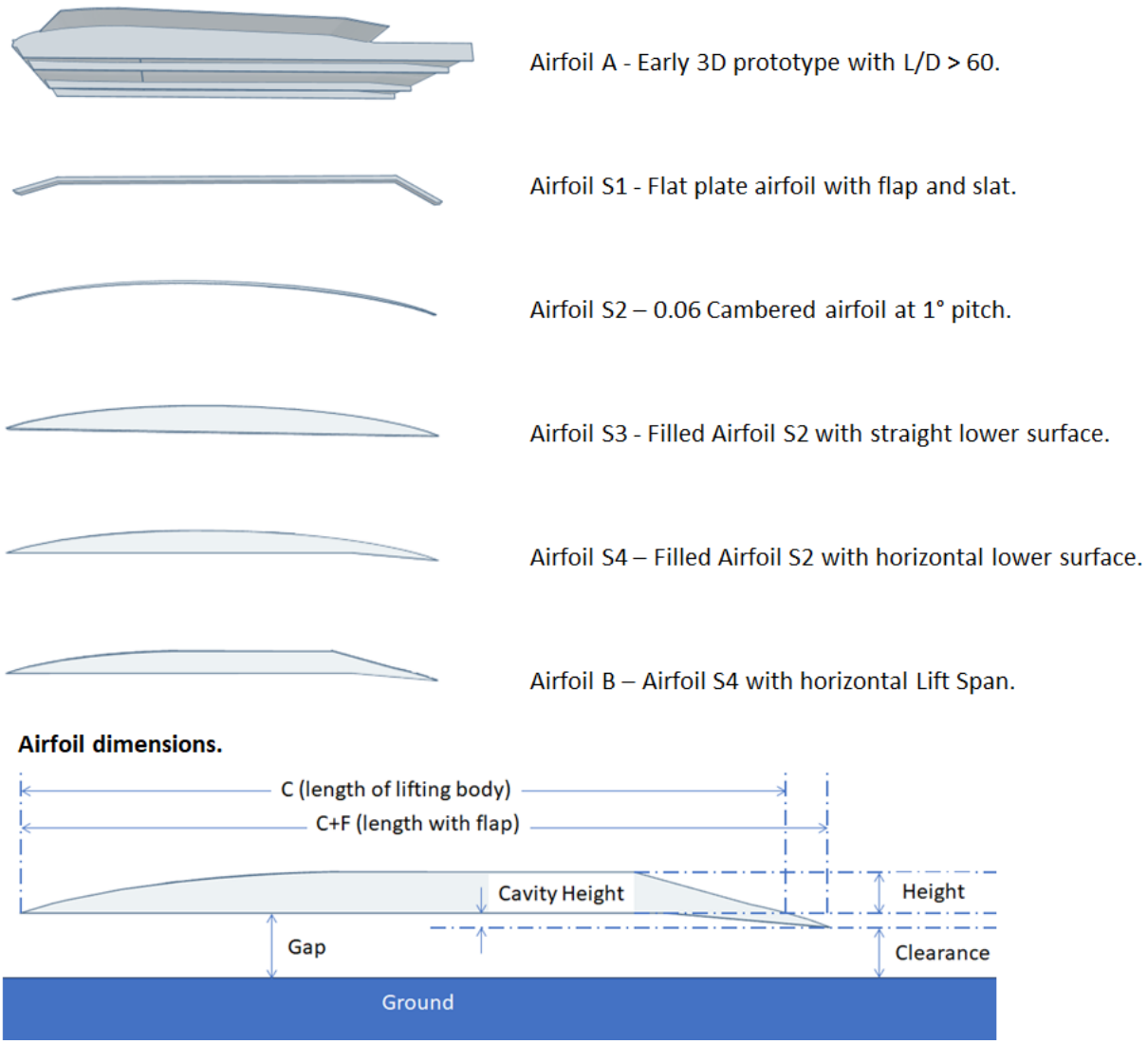

Figure 10. Airfoils studied in this paper including surrogates S1 through S4 and fuselage A and B.

Results

Trailing Flap in Ground Effect – Principles 1 and 3 identify the prospect that a trailing flap, or similar surface, can generate higher pressures and those higher pressures can extend forward throughout the entire lower surface. The trailing flap is a constant design feature in ground effect in 2D simulation of this paper where: a) the ground blocks downward loss of lift pressures, b) lateral losses are not considered, and c) proximity to the ground causes horizontal air flow that assures the converging of air flow with the trailing flap.

Figure 3 illustrates how the pressure below an airfoil increases as the airfoil approaches the ground and the air blocks downward losses of pressure; both pressure and L/D

increase as the clearance decreases. Figure 3 clearly identifies that the ground can increase L/D in excess of 100%.

Per Figure 5, a Flap% beyond that generating the highest L/D will continue to generate more lift, but at the cost of higher drag per Guideline 4. The flap setting emerges as a key control surface to create higher lift at lower velocities at the cost of higher drag, much like flap settings on today's commercial airliners.

To better understand the ability and limitations of the trailing flap in ground effect, Airfoil S1 was evaluated with and without a flap.

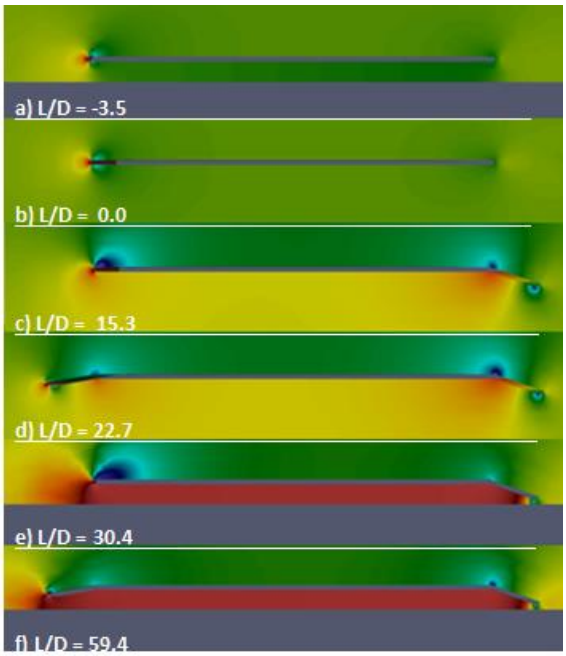

Figure 11. Pressure profiles of Airfoil S1 based slat and flap options.

Slats, Forward-Section Induced Thrust, and Cambered Airfoils– Figure 9 summarizes pressure profiles of a flat plate with and without: ground effect, a flap, and both a flap and a slat.

For the flat plate in ground effect (Figure 11a), a negative lift and L/D is the result of a negative lower pressure region forming at the leading section of the lower surface and expanding rearward. The lower pressure region forms due to the pressure of the forward stagnation point expanding downward.

The highest L/D was exhibited by the airfoil with a slat and trailing flap in ground effect with an L/D 160% greater than in the absence of ground effect. When distant from the ground, lift pressures of the lower surface dissipate leading to form drag on the lower side of the slat rather than "induced thrust". The extent of this transition is dependent on the size and shape of the slat.

The addition of flaps and slats to an airfoil is effectively the addition of camber to an airfoil, and the Figure 11 airfoils are types of thin plate cambered airfoils. Thin plate cambered airfoils were studied in detail with the Figure 10 summary of key findings.[17]

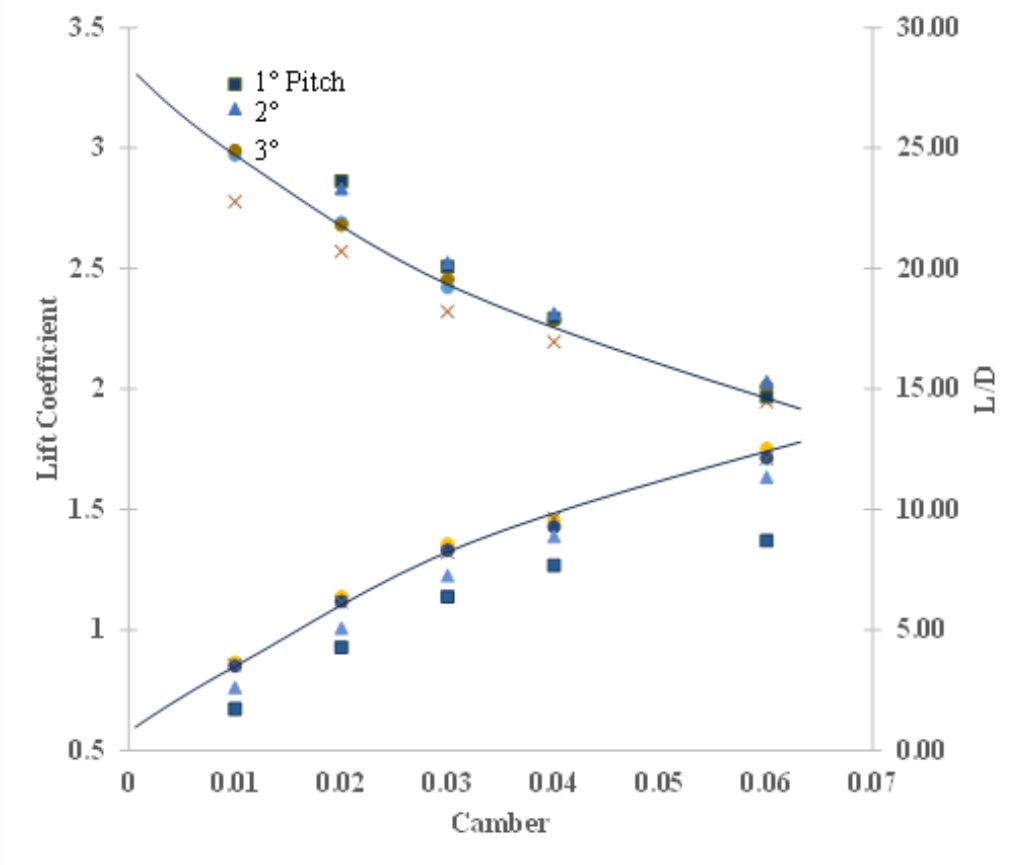

Figure 12. Impact of camber on lift coefficients and L/D on Airfoil S2.

For a higher-camber thin cambered airfoil, the thickness of the airfoil is substantially less than the height. The likely explanation for the decrease in L/D with increasing camber for the 2D simulations is the increased form drag above the trailing airfoil section. The extent to which induced thrust of the forward section can compensate for induced drag of the aft section tends to decrease as height and/or thickness increase.

The 0.06 camber airfoil, Airfoil S2, was selected for further study due to the higher lift coefficients at 0.06 camber versus lower cambers. While the L/D efficiency is less than with lower cambers, ground effect should increase this L/D by blocking the vertical loss of lift pressures. As summarized by Figure 13, the ground effect increased L/D values; demonstrating L/D in excess of 90 for the 2D airfoils.

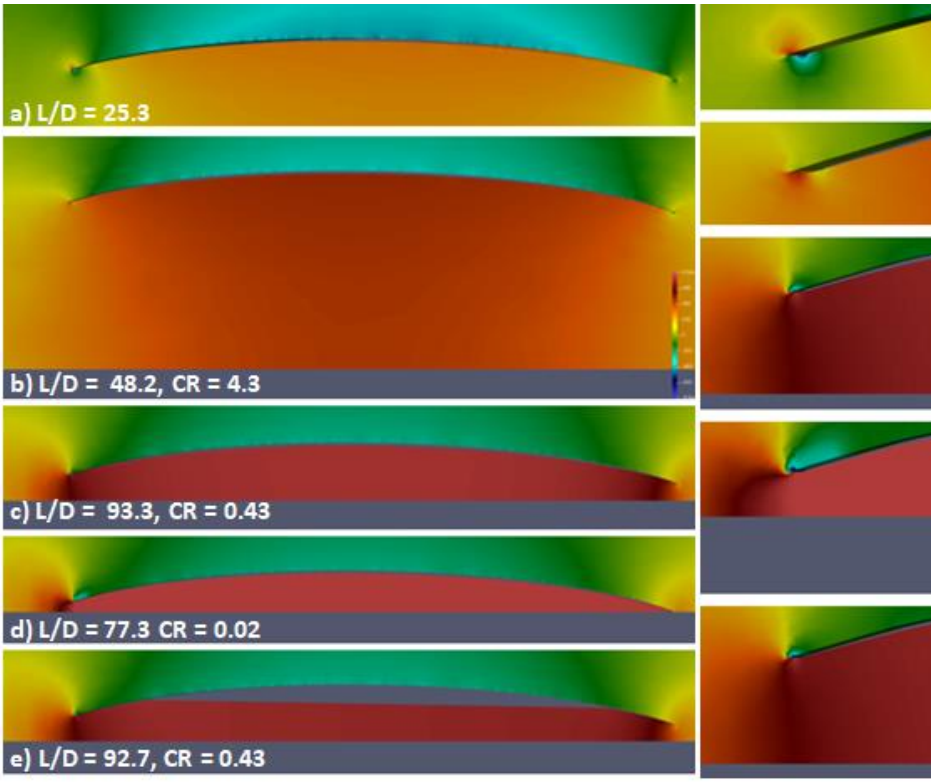

Figure 13. Pressure profiles of study on simple 0.06 camber airfoil at 1° pitch.

Each airfoil of Figure 13 has an expanded view of the leading edge. For the middle profile (CR = 0.43), the lower surface of the leading edge has higher pressures and the upper surface has a lower pressure. Hence, the lift pressures on both upper and lower surfaces at the leading edge cause both lift and thrust. This feature, referred to as leading edge "induced thrust," has been a necessary characteristic to provide higher L/D efficiencies. Induced thrust subtracts from the denominator of L/D, and so, as L/D efficiency increases induced thrust has a higher and higher impact toward achieving further increased L/D.

The slat of the flat plate airfoil provides induced thrust, leading to a higher L/D for the flat plate airfoil with a slat versus the airfoil without a slat. The cambered airfoil has a greater forward surface for induced thrust and a respective ability to attain higher L/D efficiency.

Advantages of a thin camber lifting body design include:

- Use of ultra-light weight panels or sheets for large sections of the lifting body.
- Use of bifacial solar panels for large sections of the lifting body.
- Compatibility with designs allowing for lateral and/or longitudinal expansion of the lifting body area.

The latter advantage can be of particular utility for marine applications where retraction of sections creates a robust structure for prolonged exposure to waves. The expanded structure provides increased lift to enable flight, which would be faster and possibly more energy efficient for transit than through the water.

The highest L/D efficiency for the cambered plate is when the pressure is essentially constant throughout the lower surface and the induced thrust cancels the drag of the lower surface in entirety except for the flap. This teaches to a design where the lower surface is a horizontal surface to avoid conditions where lower pressures on the lower surface leads to drag such as illustrated by Figure 13a.

Filled-Camber Prototype – While the partially-filled camber of the Figure 13e airfoil has minimal impact on L/D efficiency, the data suggest that a completely-filled camber can eliminate lower pressures on the camber's lower surface. Airfoils S3 and S4 emerge; one with a horizontal lower surface and one with a surface that is flat from leading to trailing edge. The performances are summarized by pressure profiles of Figure 14.

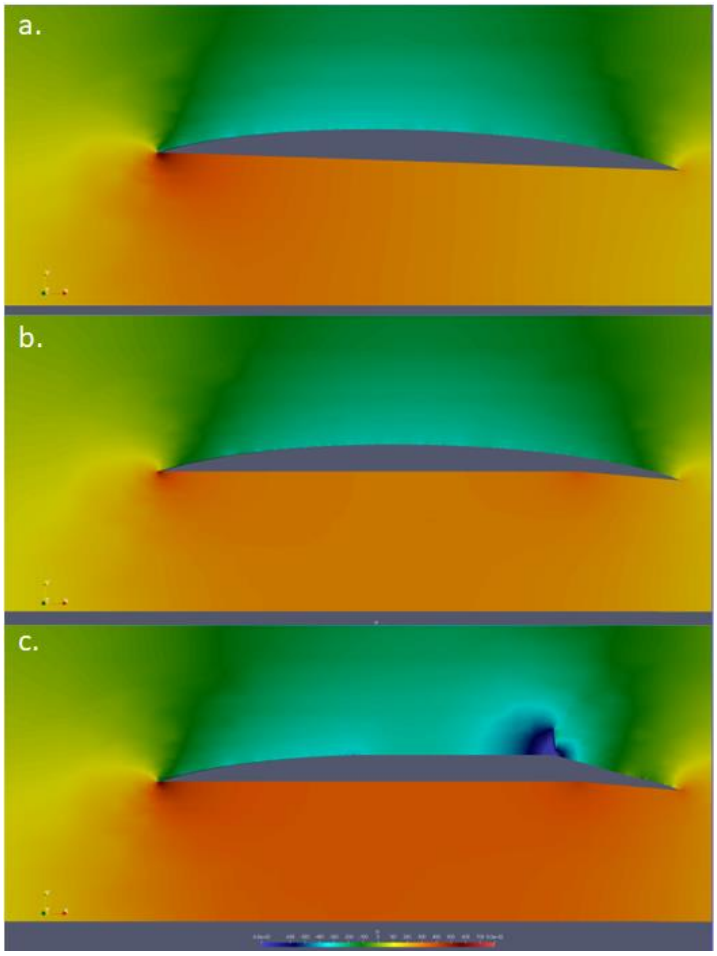

Figure 14. Pressure profiles of Airfoils S3, S4, and B (all at 1° pitch) with a Source at 2.5 m^4/s^2 on Airfoil B.

The pressure profiles identify that the horizontal lower surfaces (Airfoil S4 and Airfoil B) have more-evenly distributed pressure profile on the lower surface. A larger leading

edge stagnation region for the edge-to-edge fill diverts more on-coming air downward, leading to the higher-pressures being more forward where the pressure more-readily dissipated forward and upward. Another reason the higher performance of the horizontal fill, at the cruising condition, is increased control via the trailing flap.

Figure 15 summarizes the pressure profiles of a 0.1 t/c, also 0.1 camber, airfoil at three Source settings and expanded scales. Table 2 summarizes the data. Boundary layer separation occurred at S = 0, but was alleviated at S = 1 m^4/s^2. When adjusted for the clearance ratio, the L/D performance is the highest of the airfoils reported in this research.

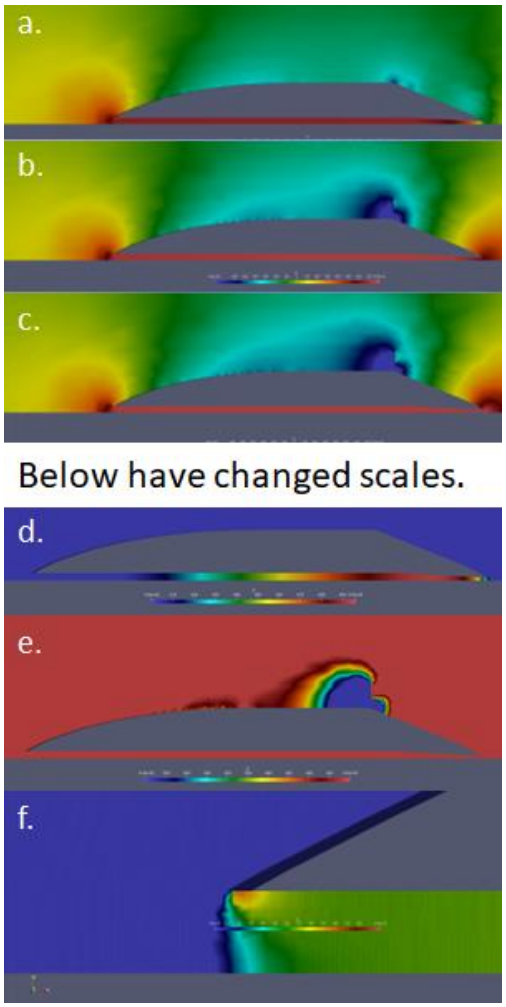

Figure 15. Pressure profiles for 0.1 t/c cambered version of Airfoil B at 0.57° pitch with Source at 0, 2.5, and 5 m^4/s^2 (a. through c.) and expanded scales for lower, upper, and leading-edge pressure scales at S=5.

Table 2. Summary of Airfoil B performances of Figure 15 pressure profiles. Airfoil dimensions prior to 0.57° pitch were L=1 m and H = 0.1m. Cavity height = 0.0035 m (prior to pitch). Clearance is 0.006 m.

S (m4/s2)	L/D	Cl	Drag Ratio (pres/visc)
0.00	26.7	1.07	9.4
1.00	60.0	1.23	3.8
2.50	76.0	1.29	2.8
5.00	114	1.40	1.7

A performance characteristic resulting in the high L/D is the lower-surface leading-edge stagnation point summarized by Figure 15f. A leading-edge stagnation point on a horizontal lower surface causes to an exceptionally-low leading section drag. The pressure drag of Table 2 reduced markedly with elimination of the boundary layer separation and continued to decrease as the stagnation point migrated lower on the leading section with increasing Source power.

The low-pressure intake of the Source literally depletes the upper region of the leading-edge stagnation region of both air and pressure. At the same time, the Source causes the formation of a powerful trailing-edge stagnation region, and that trailing-edge stagnation region facilitates the increasing of pressure in the cavity. An optimal combination of trailing taper and Source results in near-free-stream average pressure on the taper with a robust trailing-edge stagnation point.

The expanded color scales of Figure 15d and 15e allow the average lift pressures to be estimated; these estimates are 865 and -400 m^2/s^2 for Airfoils B. Based on a dynamic pressure of 800 m^2/s^2 and discarding the impact of near-free-stream pressure on the taper, these lift pressures substantiate the C_l = 1.40 of Table 2.

Airfoil B is a viable design for lifting-body fuselages. The optimal height and t/c will depend upon application and is the subject of further discussion in a separate paper.

3D Prototypes and Simulations – Airfoils S2 (simple camber) was evaluated in lifting bodies having: a) no fence, b) a fence with a lower edge at 1° pitch, and c) a fence with a lower edge at 0° pitch. Midline cross sections of the airfoil are provided by Figure 16 with additional data summarized by Table 3. The L/D = 52.1 is for a 3D digital prototype at an aspect ratio of 0.4.

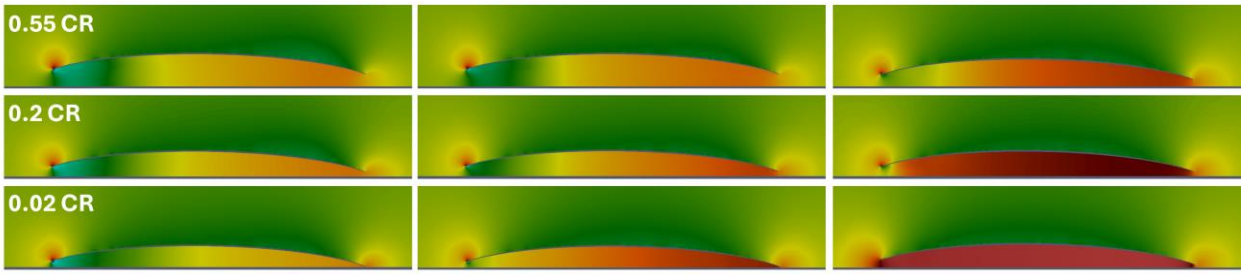

Figure 16. 3D prototype simulations at indicated CR and (from left to right) no fence, fence at 1° pitch, and fence at constant clearance. The chord pitch is 1°. Aspect ratio is 0.4.

Table 3. Performance of simple camber lifting body with two fence options and no source.

	L/D		
	Simple Camber	Angled Flush Fence	Level Fence
0.55 CR	4.4	5.5	10.2 (0.2 CR about 0.3 GR
0.2 CR	4.4	7.1	17.8 (0.1 CR with 0.2 GR)
0.02 CR	4.3	12.1	52.1

The L/D = 52.1 approaches an L/D of 57, which is the L/D of a lift force on a surface at 1° pitch. A constant clearance ratio of 0.02 was sufficient to preserve the lift force and attain this high performance; this is consistent with how the cavity pressure of the Figure 6 3D prototype approached cavity pressure of its 2D airfoil at low clearance ratios. A fence with a lower edge at 1° pitch experienced considerable losses, reducing the L/D to 12.1 at similar conditions.

Additional 3D simulations were performed to on the “Level Fence” lifting body of Table 3 with the fences extending forward as summarized by Figure 17. The L/D=52.1 was not impacted by the forward extension of the fence.

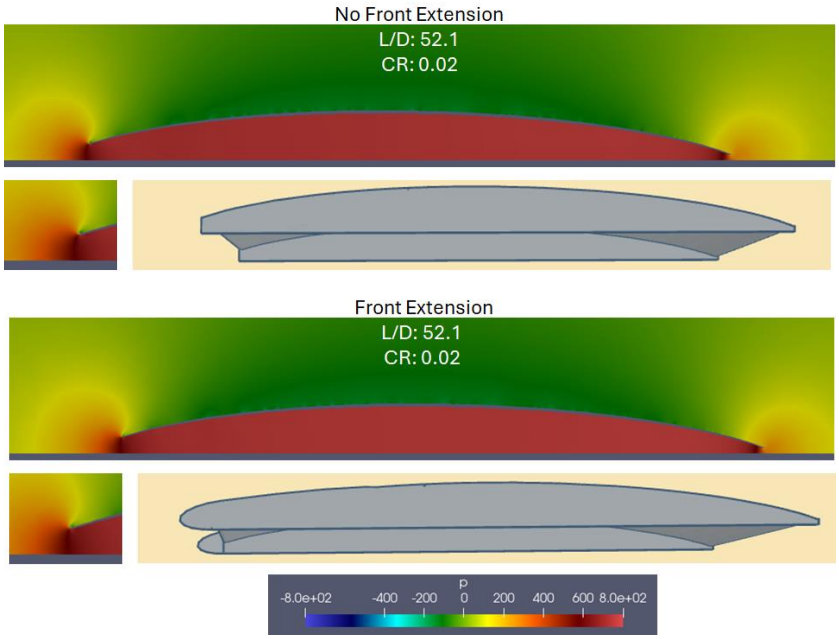

Figure 17. 3D performance of forward-extending fence for Level Fence version of Airfoil S2 at a clearance ratio of 0.02.

Figure 18 summarizes the impact of a different version of a forward-extending fence at a clearance ratio of 0.2. With the forward extension the L/D was 8.3 versus 8.6 without the forward extension. The lower L/D versus Figure 7 is due to the higher clearance ratio. At this higher clearance ratio, form drag is expressed under the lower surface of the frontal section of the thin cambered airfoil; for the Figure 17 airfoil the lower surface of the frontal section had induced thrust rather and form drag. Maximizing induced thrust is critical to attain higher L/D efficiencies.

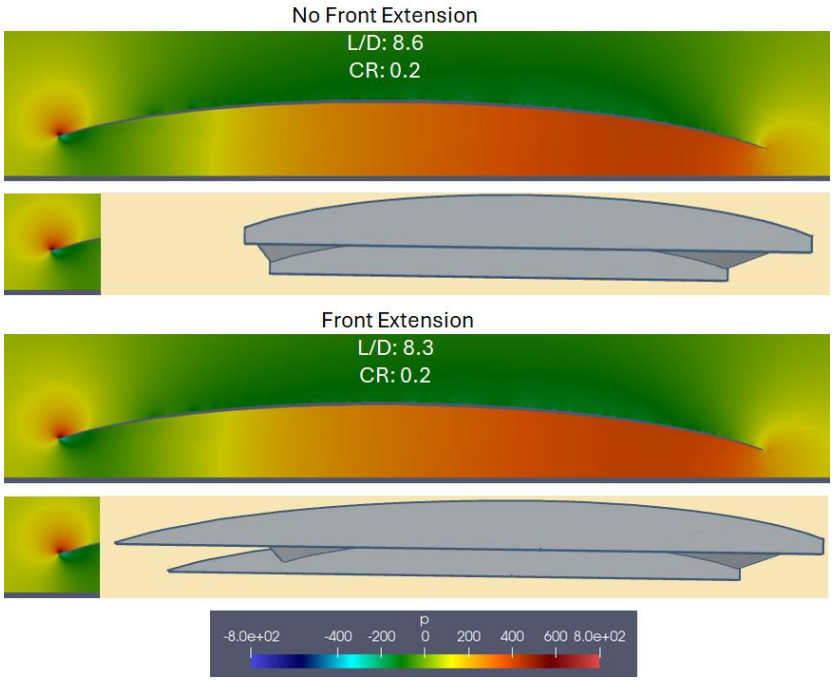

Figure 18. Additional 3D performance pressure profiles on the impact of a forward-extending fence.

Impact of Delta Configuration – The default configuration for all 3D prototypes of this research is straight versus delta. Figure 19 illustrates 3D prototype pressure profiles that compare delta versus straight frontal sections. Use of a delta configuration had minimal impact. The bottom views of the pressure profiles show well-developed lift pressures in the cavity absent form drag in the frontal sections of the cavity. Maximizing induced thrust and a clearance ratio of 0.02 led to good L/D values of 47.6 and 47.3. These performances were without Source power; induced thrust is commonly expressed on wings without the Source intake impacting pressure profiles.

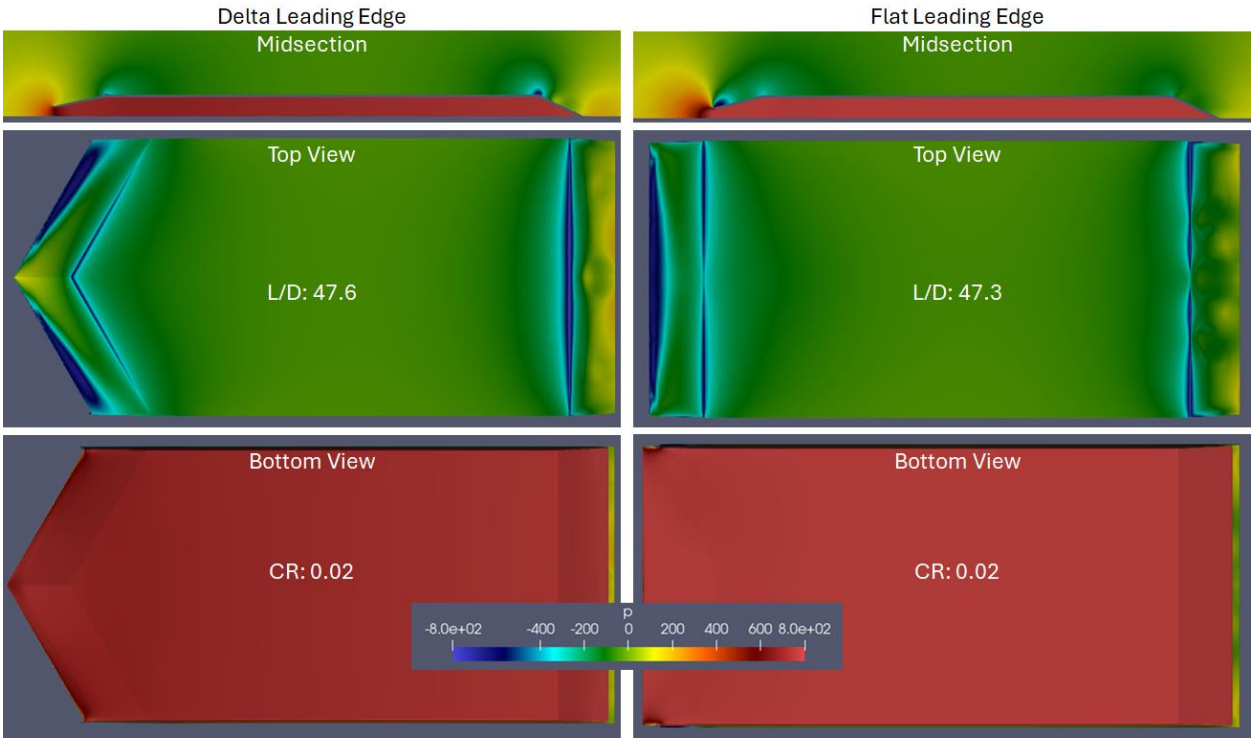

Figure 19. 3D performance of Delta.

Discussion

The attaining of high L/D efficiencies for the airfoils and digital prototype of this paper can be attributed to applications of six principles of physical science to provide simple explanations of how air flow's interactions with surfaces creates lift pressures and how surfaces and their orientations can create high L/D and block loss of lift pressures. Ground-effect aircraft are able to achieve higher L/D efficiencies because of the ground's unique ability to block the downward dissipation of lift pressures

Surrogate flat plate and simple camber airfoils provide insight and guidance to attain L/D efficiencies in excess of 50 for 3D digital prototypes. The used of a "filled" camber with a cruising-configuration horizontal lower surface inherently prevents form drag from forming on the lower surface of the camber, resulting in 3D prototypes with the best performance and thickness suitable for payloads.

Research continues to match GEFT resulting from this work with applications in railway, subway, highway, and waterway corridors.

Conclusions

Airfoils using the GEFT lower cavity were consistently able to achieve L/D in excess of 60, and 3D prototype lifting bodies were able to achieve L/D over 50 at 0.02 clearance ratios. These performances were achieved with the following features:

- A trailing-edge flap-like device behind a horizontal lower surface, collectively, defining a lower surface having an effective pitch of 0.57° to 1° at the cruising configuration.
- Cavity fences having clearance ratios near 0.02.

- A leading edge surfaces operating at maximum induced thrust in lieu of form drag.
- A trailing taper operating at average near-free-stream upper-surface pressure and absent boundary-layer separation.
- A Lift Span extending >0.4c at <1° surface pitch immediately before the trailing taper.

A flat/horizontal-bottom camber airfoil was particularly effective in attaining this performance where the forward stagnation point migrates to the horizontal surface immediately behind the leading edge.

At higher thickness ratios, an upper-surface Source between the Lift Span and trailing taper is able to mitigate boundary layer separation which may occur above the trailing taper, but the "gain:loss" ratio of gains due to reduced drag versus losses of induced thrust from the Source's air-momentum mechanism are not certain. A suggest indicator of beneficial gain:loss ratios for the Source power, toward increasing L/D, is a ratio of pressure to viscous drag >0.15.

These high performances can be victims of "weakest links", which means all the above features must be present. L/D efficiencies decreased as the fence clearance increased. Extension of fences forward and use of a delta leading-section configuration did not significantly improve performance; however, studies were not sufficiently thorough to identify that these features could not improve performance. Both the fence configuration and the wing sweep can be treated as results-driving design parameters toward optimization, and there is insufficient evidence that the evaluated fences and leading-edge sweeps were optimal.

Earlier work showed that L/D > 50 could be attained on a relatively low t/c airfoil with Source power, two pairs of fences, and a clearance ratio of 0.02. This work identified that L/D > 50 can be attained without a Source and only one pair of fences. Use of Sources and multiple pairs of fences should extend practical applications having L/D >50, which is more than 3X the average efficiency of airliners. These high L/D efficiencies are attainable in ground effect at aspect ratios >0.6.

Author Contributions

The authors confirm contribution to the paper as follows: study conception and design: G. Suppes and A. Suppes; data collection: G. Suppes and A. Suppes. Author; analysis and interpretation of results: G. Suppes and A. Suppes; draft manuscript preparation: G. Suppes and A. Suppes. All authors reviewed the results and approved the final version of the manuscript.

References

[1] Leishman, G.J., "Principles of Helicopter Aerodynamics with CD Extra," Cambridge University Press, 2006, pp. 230.

[2] Martinez-Val, R., Perez, E., and Palacin, J.F., "Historical Evolution of Air Transport Productivity and Efficiency," *Aerospace Sciences Meetings,* Vol. 43, 2005, https://doi.org/10.2514/6.2005-121

[3] Fleck, A., "Chart: Which mode of transport is the most polluting?" *Statista,* 2024,

[4] McIver, J.B., "Cessna Skyhawk II / 100 Performance Assessment," 2003.

[5] Arif, N., "Performance Analysis of B-2 Spirit," 2023.

[6] Szondy, D., "DARPA's ground-effect X-plane will haul 100 tons of cargo," *New Atlas,* 2024, https://newatlas.com/military/darpas-liberty-lifter-x-plane-gets-a-face-lift/

[7] Deviparameswari, K., Meenakshi, S., Akshay Kumar, N., Vigneshwaran, R., Rohini Janaki, B., Vinsiya Maria, A., Keerthana, N., Surya, B., Vetrivel, M., Thianesh, U.K., Rajarajan, S., Manikandan, P., "The Effects of Ground Clearance and Boundary Layer Blockage Factor on the Aerodynamics Performance of the Hyperloop Pod and Transonic Ground-Effect Aircraft | AIAA AVIATION Forum," *AIAA Aviation Forum,* 2021, https://doi.org/10.2514/6.2021-2586

[8] Qu, Q., Wang, W., Liu, P., and Agarwal, R.K., "Airfoil Aerodynamics in Ground Effect for Wide Range of Angles of Attack," *AIAA Journal,* Vol. 53, No. 4, 2015, https://doi.org/10.2514/1.J053366

[9] Suppes, A., and Suppes, G., "New Benchmarks in Ground-Effect Flight Energy Efficiency," [online database]July 10,2024https://www.researchsquare.com/article/rs-4707178/v1 [cited Jul 29, 2024].

[10] Suppes, A., and Suppes, G., "Supplemental Documents in Various Stages of pre-print publication and review," 2024, https://hs-drone.com/resources

[11] Suppes, G., and Suppes, A., "Ground Effect Vehicle," Vol. PCT/US24/35242, 2024, pp. 1-32. www.hs-drone.com

[12] Klose, B., Spedding, G., and Jacobs, G., "Direct numerical simulation of cambered airfoil aerodynamics at Re = 20,000," 2021, https://doi.org/10.48550/arXiv.2108.04910

[13] Michna, J., and Rogowski, K., "Numerical Study of the Effect of the Reynolds Number and the Turbulence Intensity on the Performance of the NACA 0018 Airfoil at the Low Reynolds Number Regime," *Processes,* Vol. 10, 2022, pp. 1004. 10.3390/pr10051004

[14] Serrano, J., Tiseira, A., García-Cuevas, L., and Varela, P., "Computational Study of the Propeller Position Effects in Wing-Mounted, Distributed Electric Propulsion with Boundary Layer Ingestion in a 25 kg Remotely Piloted Aircraft," *Drones,* Vol. 5, 2021, pp. 56. 10.3390/drones5030056

[15] McCabe, Tom COO & GC, Istari Digital, Inc., "Conversation," 2024, https://www.istaridigital.com/

[16] Suppes, A., and Suppes, G., "Thermodynamic Analysis of Distributed Propulsion," *Research Square,* 2023, pp. 1-26. 10.21203/rs.3.rs-4670270/v1

[17] Suppes, G., and Suppes, A., "Understanding Thin Cambered Airfoils and their Solar Aircraft Applications," *Research Square,* 2023, pp. 1-29. https://doi.org/10.21203/rs.3.rs-4670250/v1

[18] Garcia, R., and Siewert, C., "The linearized Boltzmann equation: Sound-wave propagation in a rarefied gas," *Zeitschrift Fur Angewandte Mathematik Und Physik,* Vol. 57, 2005, pp. 94-122. 10.1007/s00033-005-0007-8

[19] Loyalka, S.K., "Motion of a sphere in a gas: Numerical solution of the linearized Boltzmann equation," *Physics of Fluids: Fluid Dynamics,* Vol. 4, No. 5, 1992, pp. 1049-1056. 10.1063/1.858256

[20] Loyalka, S.K., and Chang, T.C., "Sound-wave propagation in a rarefied gas," *Physics of Fluids,* Vol. 22, 1979, pp. 830.

[21] Loyalka, S., "On Boundary Conditions Method in the Kinetic Theory of Gases," *Zeitschrift Naturforschung Teil A,* Vol. 26, 2014, pp. 1708. 10.1515/zna-1971-1020

[22] Suppes, A., and Suppes, G., "Highly-Efficient Low-AR aerial vehicles in urban transit," *Proceedings of the 2014 Transportation Research Board Annual Meeting,* January, 2024.